the effective conversion by ZrO_2 to zirconates at moderate temperatures. A great deal has also been learned about ways in which ZrI_4 can be sequestered in reduced zirconium iodide phases, particularly those such as $Zr_6I_{12}C$ that are greatly stabilized by a common impurity such as carbon.[2,11]

The actual detection of cesium zirconates (as well as probable zirconium iodide phases) in used fuel rods has not been accomplished unambiguously. This process is made difficult not only by the intense radiation present but also by the high proclivity of both types of products to hydrolysis. The latter factor has generally not been taken into consideration in postfission examinations of fuel rods.

Acknowledgment. We are particularly indebted to Professor R. Hoppe for his interest in this work and for his provision of both the MAPLE calculations and information on related research that has taken place at Giessen. We also acknowledge the continuing provision of X-ray diffractometer facilities by Professor R. A. Jacobson.

Supplementary Material Available: Tables of anisotropic thermal ellipsoid parameters for the atoms in Cs_2ZrO_3 (1 page); table of observed and calculated structure factors for Cs_2ZrO_3 (1 page). Ordering information is given on any current masthead page.

Preparation of Boron-Containing Ceramic Materials by Pyrolysis of the Decaborane(14)-Derived $[-B_{10}H_{12}{\cdot}Ph_2POPPh_2]_x-$ Polymer

Dietmar Seyferth,*,† William S. Rees, Jr.,† John S. Haggerty,*,‡ and Annamarie Lightfoot‡

Department of Chemistry and Materials Processing Center, Massachusetts Institute of Technology, Cambridge, Massachusetts 02139

Received June 13, 1988

The pyrolysis of the known polymer $[-B_{10}H_{12}{\cdot}Ph_2POPPh_2]_x-$ to give a boron-containing ceramic has been studied. The pyrolysis to 1000 °C gives an amorphous solid in 93% ceramic yield that contains boron, phosphorus, oxygen, and a large excess of carbon. Further studies devoted to this material have served to characterize it with respect to surface area, pore size and distribution, density, grain size, crystalline phases, and elemental composition as a function of temperature up to 2350 °C.

Introduction

Polymer pyrolysis as a route to ceramic materials has received much attention in recent years.[1] This procedure has been applied principally to the preparation of silicon-containing ceramic materials such as silicon carbide, nitride, carbonitride, and oxynitride.[1,2] Much less work has been devoted to the application of polymer pyrolysis to the preparation of boron-containing ceramic materials. The few reports in this area have dealt mostly with boron nitride precursors,[3] and there is only one recent example of the preparation of boron carbide by the preceramic polymer route.[3h]

The development of polymer pyrolysis as a route to ceramics beyond the restricted field of pyrolytic carbon came about as a result of interest in new "high-technology" applications of ceramics with exceptional high-temperature properties such as the carbides, nitrides, and oxides of silicon, boron, aluminum, and the early transition metals. For instance, there is considerable interest in strong ceramic fibers for use in composites, in inert ceramic coatings for materials that are subject to high-temperature oxidation and other forms of corrosion, and in low-loss binders for use in forming ceramic powders into shaped bodies. These applications require a soluble or fusible polymeric precursor that can be spun into fibers and/or that can be used to coat ceramic bodies and powder particles. Also of interest is the preparation of shaped ceramic bodies by pyrolysis of shaped bodies of such "preceramic" polymers.

The issues that are of importance in preceramic polymer design and preparation have been discussed.[1] The most important *chemical* issues are those of polymer processability, high ceramic yield, and elemental composition. However, there are important *ceramics* issues as well, such

† Department of Chemistry.
‡ Materials Processing Center.

(1) Reviews on preceramic polymers: (a) Wynne, K. J.; Rice, R. W. *Ann. Rev. Mater. Sci.* **1984**, *14*, 297. (b) Rice, R. W. *Am. Ceram. Soc. Bull.* **1983**, *62*, 889. (c) Seyferth, D. In *Transformations of Organometallics Into Common and Exotic Materials: Design and Activation*; NATO ASI Series E: Applied Sciences, 141; Laine, R. M., Ed.; Martinus Nijhoff: Dordrecht, 1988; pp 133–154. (d) Seyferth, D.; Wiseman, G. H.; Schwark, J. M.; Yu, Y.-F.; Poutasse, C. A. In *Inorganic and Organometallic Polymers*; ACS Symposium Series 360; Zeldin, M., Wynne, K. J., Allcock, H. R., Eds.; American Chemical Society: Washington, D.C., 1988; pp 143–155.

(2) (a) Yajima, S. *Am. Ceram. Soc. Bull.* **1983**, *62*, 893. (b) Wills, R. R.; Markle, R. A.; Mukherjee, S. P. *Am. Ceram. Soc. Bull.* **1983**, *62*, 904. (c) Schilling, Jr., C. L.; Wesson, J. P.; Williams, T. C. *Am. Ceram. Soc. Bull.* **1983**, *62*, 912. (d) LeGrow, G. E.; Lim, T. F.; Lipowitz, J.; Reaoch, R. S. *Am. Ceram. Soc. Bull.* **1987**, *66*, 363. (e) Laine, R. M.; Blum, Y. D.; Tse, D.; Glaser, R. In *Inorganic and Organometallic Polymers*; ACS Symposium Series 360; Zeldin, M., Wynne, K. J., Allcock, H. R., Eds.; American Chemical Society: Washington, D.C.; 1988; pp 124–142.

(3) (a) Narula, C. K.; Schaeffer, R.; Paine, R. T.; Dayte, A., Hammetter, W. F. *J. Am. Chem. Soc.* **1987**, *109*, 5556. (b) Narula, C. K.; Janik, J. F.; Duesler, E. N.; Paine, R. T.; Schaeffer, R. *Inorg. Chem.* **1986**, *25*, 3346. (c) Wada, H.; Ito, S.; Kuroda, K.; Kato, C. *Chem. Lett.* **1985**, 691. (d) Pacioreck, K. J. L.; Kratzer, R. H.; Harris, D. H.; Smythe, M. E.; Kimble, P. F. U.S. Patent 4581468, 1986. (e) Pacioreck, K. J. L.; Harris, D. H.; Kratzer, R. H. *J. Polym. Sci., Polym. Chem. Ed.* **1986**, *24*, 173. (f) Lindemanis, A. E. *Mater. Sci. Res.* **1984**, *17*, pp 111–121. (g) Rees, Jr., W. S.; Seyferth, D. *J. Am. Ceram. Soc.* **1988**, *71*, C-194. (h) Mirabelli, M. G. L.; Sneddon, L. G. *J. Am. Chem. Soc.* **1988**, *110*, 3305.

0897-4756/89/2801-0045$01.50/0

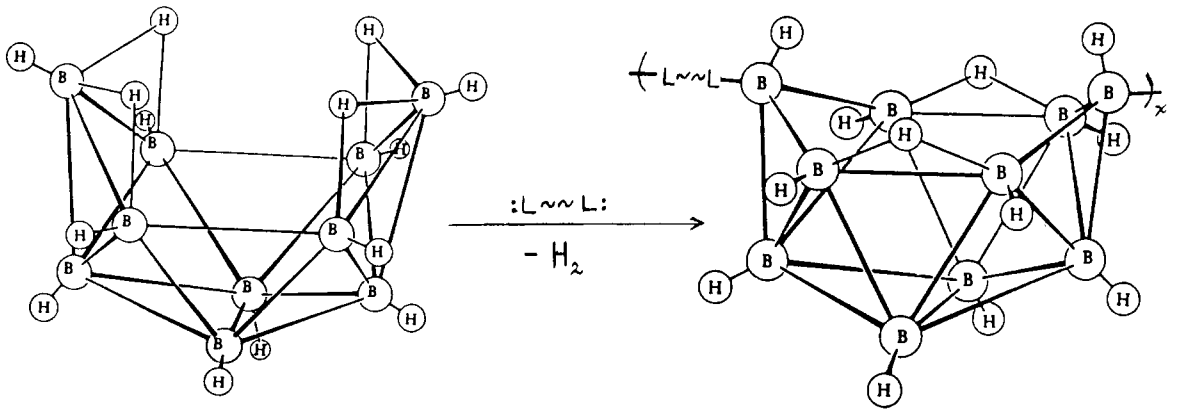

(1)

as control of porosity and microstructure.

Boron carbide, B_4C, is of considerable interest because of its high thermal stability (mp 2450 °C), high hardness, and resistance to attack at high temperature by many chemicals.[4] The investigation described here had as its objective the synthesis of a polymeric precursor for boron carbide, either as the pure material or as a major component of a ceramic blend.

Results and Discussion

Synthesis and Preliminary Studies. As a starting material for this investigation we chose decaborane(14), $B_{10}H_{14}$, since it is a difunctional molecule with respect to reaction with Lewis bases (:L), forming products of the type $L{\cdot}B_{10}H_{12}{\cdot}L$ with concomitant loss of 1 mol equiv of dihydrogen.[5] With difunctional Lewis bases (:L~~L:), linear polymers are formed (eq 1). Decaborane(14)-derived polymers had been prepared some 20 years ago by Parshall[6] and by Schroeder and co-workers,[7] both using diphosphines as the difunctional Lewis bases. In the formation of such $L{\cdot}B_{10}H_{12}{\cdot}L$ adducts, monomeric or polymeric, there is no polyhedral rearrangement of boron atoms, the only structural change being relocation of B–H–B three-center, two-electron bonds on going from the nido to the arachno structure.

For detailed investigation of polymer pyrolysis as a route to boron-containing ceramics we chose the $[-B_{10}H_{12}{\cdot}Ph_2POPPh_2]_x-$ polymer that had been prepared first by Schroeder and co-workers by hydrolysis of $ClPh_2P{\cdot}B_{10}H_{12}{\cdot}PPh_2Cl$ with wet benzene in the presence of triethylamine or by reaction of this adduct with $HOPh_2P{\cdot}B_{10}H_{12}{\cdot}PPh_2OH$ in the presence of triethylamine.[7a,b] This polymer, an air-stable, white solid with mp >300 °C, is soluble in polar organic solvents such as acetonitrile and *N,N*-dimethylformamide (DMF) and was found to have a molecular weight of 27 000 (light scattering, in *N*-methylpyrrolidone solution). When this polymer was heated to 350 °C, 4 mol equiv of dihydrogen was evolved per $B_{10}H_{12}$ unit, as well as a trace amount of benzene. The residue was insoluble in all organic solvents tried. Pyrolysis at higher temperature was not investigated by Schroeder and co-workers.

We have found that pyrolysis of the $[-B_{10}H_{12}{\cdot}Ph_2POPPh_2]_x-$ polymer, prepared as described by Schroeder and co-workers, in a stream of argon to 1000 °C at 10 °C/min, gave a black powder as residue in 86% ceramic yield.[8] Elemental analysis of the pyrolysis product, which was amorphous as determined by X-ray diffraction, gave 23.7% B, 57.4% C, 11.5% P, and 0.2% H. Thus this material contains a large excess of free carbon (compare B_4C: calcd 78.26% B, 21.74% C). This was not unexpected since it is known that pyrolysis of phenyl-substituted organosilicon polymers always gives a large excess of carbon in addition to SiC.[9] Exploratory experiments showed the $[-B_{10}H_{12}{\cdot}Ph_2POPPh_2]_x-$ polymer to be potentially useful as a binder for boron carbide powder and in the formation of shaped ceramic bodies. Accordingly, it was chosen for further, more detailed studies.

The potential utility of this polymer in the formation of shaped ceramic bodies no doubt is due in large part to its extremely high ceramic yield on pyrolysis. However, a disadvantage of this polymer, already noted, is the fact that the solid pyrolysis product contains a large excess of free carbon. We have addressed this problem by forming a composite of the $[-B_{10}H_{12}{\cdot}Ph_2POPPh_2]_x-$ polymer with the amount of elemental boron powder required to convert this excess carbon to B_4C. (Elemental boron and carbon undergo reaction to form boron carbide at around 1600 °C).[4] Such an experiment (pyrolysis to 1000 °C in argon) gave a ceramic residue that contained 73.2% B, 21.3% C, and 4.18% P. Heating this material to 1500 °C in argon left a residue that now contained 76.9% B, 18.0% C, and 2.6% P. This translates to 87.3% by weight B_4C and 12.7% by weight B if one assumes only the presence of boron and carbon and ignores the small amounts of phosphorus and oxygen still present. Examination of this material by powder X-ray diffraction (XRD) showed the presence of crystalline B_4C.

During the course of this investigation other $[-B_{10}H_{12}{\cdot}\text{diphosphine}]_x-$ polymers were examined for potential utility: those in which the diphosphine is $Ph_2PN{=}PPh_2CH_2CH_2PPh_2{=}NPPh_2$[7a,c] and $Ph_2PNHNHPPh_2$. These, however, gave only low ceramic yields (52% and 57%, respectively) on pyrolysis to 1000 °C and thus were not investigated further.

Characterization of Materials. Four types of samples were characterized systematically: as-fired powder (powder) and bar (bulk) samples, in addition to ground powders from either fired bars (ground bulk) or powders (ground powder) derived from the $[-B_{10}H_{12}{\cdot}Ph_2POPPh_2]_x-$ poly-

(4) (a) Thompson, R. In *Progress in Boron Chemistry*; Brotherton, R. J., Steinberg, H., Eds.; Pergamon: London, 1970; Vol. 2, pp 173–230. (b) Wentorf, Jr., R. H. In *Kirk-Othmer Encyclopedia of Chemical Technology*, 3rd ed.; Wiley: New York, 1978; Vol. 4, pp 126–127.

(5) *Gmelin Handbook of Inorganic Chemistry*, 8th ed.; New Supplement Series, *Boron Compounds 20, Boron–Hydrogen Compounds*; Springer-Verlag: Berlin, 1979; Vol. 54, pp 151–165.

(6) Parshall, G. W. U.S Patent 3035949, 1962.

(7) (a) Schroeder, H. A.; Reiner, J. R.; Knowles, T. A. *Inorg. Chem.* **1963**, *2*, 393. (b) Reiner, J. R.; Schroeder, H. A. U.S. Patent 3141856, 1964. (c) Schroeder, H. A. U.S. Patent 3155630, 1964.

(8) Percent ceramic yield = (wt pyrolysis residue × 100)/(wt pyrolysis charge).

(9) White, D. A.; Oleff, S. M.; Fox, J. R. *Adv. Ceram. Mater.* **1983**, *2*, 53.

Table I. Summary of Crystalline Phases Observed by XRD and EDS Determined Phosphorus Content in Materials Produced from the $[-B_{10}H_{12}\bullet Ph_2POPPh_2]_x-$ Polymer at Various Stages of Processing

temp, °C	time, h	sample	P (EDS)	rel peak int (XRD) B_4C	C	$B_{13}P_2$	BP
1000	0.5	bulk	yes	0	0	0	0
1500	10.0	powder		62	100	90	0
1500	10.0	bulk	yes	26	70	100	42
1500	10.0	bulk[a]		0	47	65	100
1500	25.0	bulk	yes	62	80	100	9
1500	25.0	bulk[a]		0	70	71	100
1550	0.5	bulk	yes	0	43	100	53
1870	0.5	bulk	yes	42	100	0	0
2090	0.5	bulk	no	18	100	0	0
2350	0.5	bulk	no	9	100	0	0

[a] After ~1 mm removed by surface grinding.

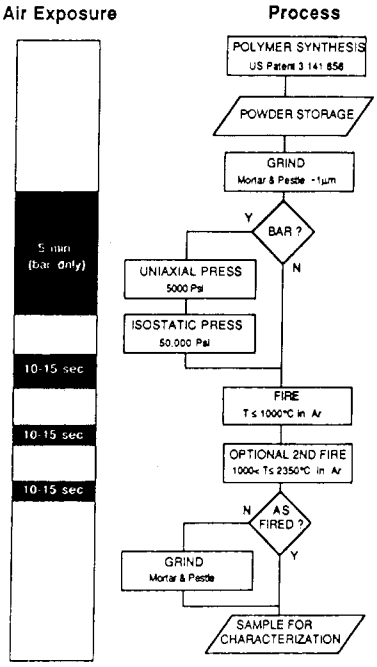

Figure 1. Summary of processing steps and air exposures for the ceramic blend produced from the $[-B_{10}H_{12}\cdot Ph_2POPPh_2]_x-$ polymer.

mer. These sample groups (Figure 1) permitted a qualitative determination of the scale over which pores were isolated; they also permitted the effect of diffusion distance on phosphorus and oxygen losses to be investigated.

Crystallinity and Grain Size. X-ray diffraction patterns were made of as-fired powder and the surfaces of bulk samples, both before and after removal of ~1 mm of exterior thickness. The results illustrate some important differences between samples fired as powder and bulk (Table I). A complex crystallization sequence that results in part from the phosphorus residuals is also evident.

No sample showed evidence of crystallinity for firing temperatures below 1500 °C. This is common for the extremely fine, sometimes microcrystalline, structures that result from polymer pyrolysis.[10] Crystalline phases emerged with progressively sharper diffraction patterns with increasing firing temperatures.

After firing at 1500 °C for 10 h, as-fired powder samples exhibited crystalline B_4C, C, and $B_{13}P_2$. Exterior surfaces of bulk samples subjected to the same firing cycle revealed these phases in addition to BP. The BP concentration increased with distance from the outer surface (Table I).

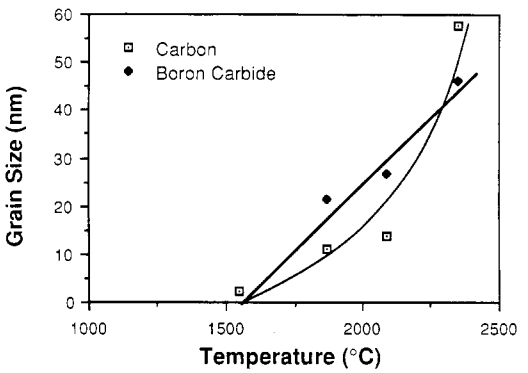

Figure 2. Growth of B_4C and C crystallite grain sizes, as determined by XRD line broadening, on the exposed surface of a bulk sample of ceramic derived from the pyrolysis of the $[-B_{10}H_{12}\cdot Ph_2POPPh_2]_x-$ polymer in an argon atmosphere after maintaining firing temperature for 0.5 h.

The initial appearance of crystalline BP at 1500 °C in these samples, its subsequent conversion to crystalline $B_{13}P_2$, and finally its disproportionation into solid boron and gaseous phosphorus as firing temperatures exceeded 1500 °C is similar to reported findings for simple mixtures of boron and phosphorus.[4]

Crystalline B_4C was first observed only on the exterior surfaces of bulk samples fired at 1500 °C. Boron carbide and carbon diffraction patterns became well developed for bulk samples only for firing temperatures of 1870 °C and higher. With heating to 2090 °C, B_4C was present throughout the bulk sample. The emergence of a diffraction peak at $2\theta = 44.6°$ with Cu Kα radiation ({101} type carbon planes) in the bulk sample fired to 2350 °C is evidence of carbon graphitization.[11] The differences in crystallinity between powder and bulk samples and between the surfaces and interiors of bulk samples probably result from enhanced phosphorus and oxygen losses in the proximity of free surfaces (Table I).

The B_4C and C crystallite sizes on the exposed surfaces of bulk samples were determined by XRD line broadening. Results for samples fired at temperatures between 1500 and 2350 °C for 0.5 h are summarized in Figure 2. Both phases grow continuously to the highest temperature investigated (2350 °C). The maximum observed grain sizes (~50–60 nm) are extremely small by comparison to materials processed by conventional techniques.[12] The BP grain size on the exposed surface of the bulk samples fired at 1525 ± 25 °C decreased from a dimension that was larger than the broadening limit of the X-ray diffractom-

(10) Walker, Jr., B. E.; Rice, R. W.; Becher, P. F.; Bender, P. A.; Coblenz, W. S. *Am. Ceram. Soc. Bull.* **1983**, *62*, 916.

(11) Jenkins, G. M.; Kawamura, K. *Polymeric Carbons—Carbon Fibre, Glass and Char*; Cambridge University Press: Oxford, 1976.

(12) Schwetz, K. A.; Grellner, W. *J. Less-Common Met.* **1981**, *82*, 37.

eter (150 nm) for a 0.5-h heat treatment to 13 nm for a 25-h heat treatment. Internal BP grain sizes also decreased with firing time but were 3–5 times larger than the surface grains. The $B_{13}P_2$ grain size remained constant (9–14 nm) with respect to both time held at 1500 °C and position throughout the bulk sample.

TEM and STEM analyses of internal regions of bulk samples heated at 1500 °C for 10 h revealed four distinct crystalline phases in an amorphous matrix; three had spherical dimensions of ~50 nm, 150–200 nm, and >1 μm, and one was 10 nm × 200 nm needles. The XRD-calculated sizes of $B_{13}P_2$ and BP (13 and 125 nm, respectively) are in general agreement with two of the observed crystalline phases. With the exception of the BP phase, the dimensions of the crystalline phases were uniform throughout the bulk sample volumes.

Composition. Chemical compositions for the $[-B_{10}H_{12}\cdot Ph_2POPPh_2]_x-$ polymer-based materials present at various stages of processing are summarized in the Experimental Section. Energy-dispersive X-ray spectroscopy (EDS) results for qualitative phosphorus content are presented (Table I). Even though the $[-B_{10}H_{12}\cdot Ph_2POPPh_2]_x-$ polymer gives a high yield of solids that include B_4C, it is evident that the pyrolysis product should be carbon rich. The B/C ratios observed for the materials fired as either powder or bulk are higher than those present in the calculated composition of a material resulting from loss of all elements present in the polymer except boron and carbon. Although the ceramic samples were carbon rich, some of the carbon initially present in the polymer was lost during pyrolysis. The determination of a nominal formulation for amorphous materials is not easily carried out. For example, it is not simple to differentiate between an intimate mixture of boron and carbon and boron carbide, when both samples contain the same elemental composition and are amorphous. If we assume that all boron is present as B_4C and the remaining carbon as the free element, then a nominal formulation may be derived for the material. For example, in this manner, the ceramic blend produced by pyrolysis of the $[-B_{10}H_{12}\cdot Ph_2POPPh_2]_x-$ polymer to 2350 °C may be represented as $(B_4C)_{1.0}(C)_{7.0}$ on a molar basis or 39.7% B_4C and 60.3% C on a weight basis. It should be stressed that this is only a *nominal* formulation of this material. It could also contain amorphous phases of nonstoichiometric boron carbide and/or elemental boron. There is not enough information available at the present time to present a realistic formula for the composition of those materials present at intermediate stages of processing. However, at this point several qualitative trends have emerged and will be pointed out. Boron carbide and carbon crystallize from the amorphous blend at ~1500 °C. Oxygen and phosphorus loss is not complete until temperatures greater than 1500 °C are reached.

The effect of the shortened diffusion distances in the powder samples is shown by comparing the phosphorus and oxygen contents of the 1500 °C powder and bulk samples (P: bulk, 11.2%; powder, 0.4%. O: bulk, 6.7%; powder, 2.9%). The effect of increased firing temperature is shown by comparing results obtained at 1000 and 1500 °C for powder samples and those obtained at 1500 and 2300 °C for bulk samples (see Experimental Section). Both shorter dimensions and increased temperature enhance phosphorus and oxygen losses.

EDS analyses of fracture surfaces (Table I) show that all detectable phosphorus is lost from the bulk samples for firing temperatures between 1870 and 2090 °C. EDS X-ray mapping of the internal phosphorus distribution within a bulk sample fired at 1500 °C for 10 h shows that the phosphorus is concentrated in isolated regions, some of which surround the ~50-nm, phosphorus-containing crystallites (Figure 3). Thus, phosphorus segregation occurs on a macroscopic level near exposed surfaces and on a microscopic level near precipitates, in bulk samples.

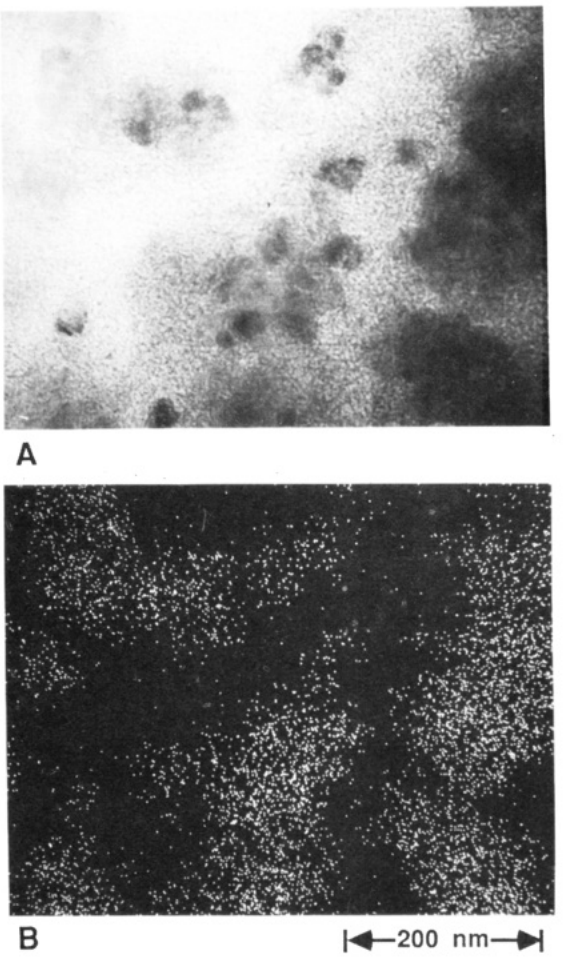

Figure 3. (A) Scanning electron micrograph of an internal cross section of a bulk ceramic sample derived from the $[-B_{10}H_{12}\cdot Ph_2POPPh_2]_x-$ polymer by pyrolysis at 1500 °C for 10 h, showing ~50-nm crystals embedded in an amorphous matrix. (B) X-ray map of phosphorus distribution in the region shown in A. Lighter areas indicate higher concentration.

Oxygen levels found in some fired samples are higher than those predicted from the polymer composition (3.2% O in the polymer). It has not been determined whether the apparent excesses are entirely real or whether they result in part from contamination of the high-surface-area materials during processing and/or chemical analyses. Air exposure during processing was minimized to reduce the contamination of processed samples with atmospheric water vapor and oxygen (Figure 1).

It is not known how oxygen is held in the ceramic blends formed by pyrolysis of this precursor. Boron oxide (mp 450 °C) and phosphorus oxide (mp 580 °C) both melt well below 1000 °C. Boron phosphate, BPO_4, is also a known material. All of these oxygen-containing compounds are either soluble in hot water or easily hydrated. However, an attempt to extract samples of the ceramic material (fired to 1000 °C as a powder) with boiling water did not result in any appreciable weight change of the samples.

The diffuse-reflectance Fourier transform (DRIFT) infrared spectra of powder samples of the $[-B_{10}H_{12}\cdot Ph_2POPPh_2]_x-$ polymer fired to 1000 and 1500 °C each showed broad absorptions at 1104–1406 cm^{-1} (maxima at

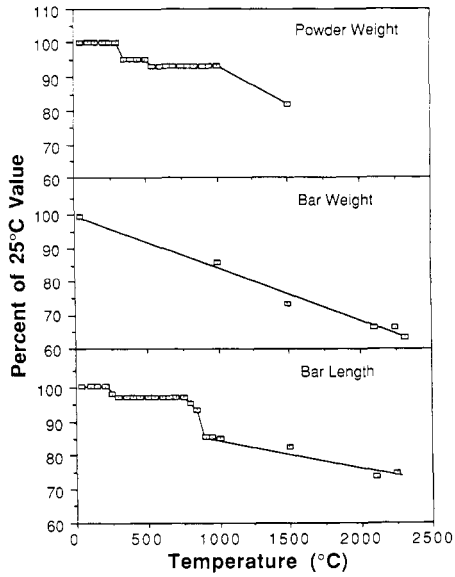

Figure 4. Graph of weight and length changes of the $[-B_{10}H_{12}\cdot Ph_2POPPh_2]_x-$ polymer as a function of temperature.

1190 and 1302 cm^{-1}; B_4C shows absorptions at 1080 and 1340 cm^{-1}).[13] The absence of DRIFT absorptions attributable to the presence of B–O and P–O bonds,[13] coupled with the water extraction mentioned above, leads us to conclude that the presence of oxygen, as determined by chemical analysis, arises from dioxygen contamination of samples during handling and that oxygen is not present on the surface of the ceramic derived from pyrolysis of the $[-B_{10}H_{12}\cdot Ph_2POPPh_2]_x-$ polymer. Additionally, samples that had been fired only to 1000 °C had absorptions at 2350–3100 cm^{-1} attributed to the presence of residual B–H and C–H bonds. From these data we conclude that processing temperatures above 1000 °C are required for complete removal of all hydrogen-containing moieties.

Density, Surface Area, and Porosity. Weight and length changes observed during firing of the $[-B_{10}H_{12}\cdot Ph_2POPPh_2]_x-$ polymer from 50 to 2350 °C are shown in Figure 4 for powder and bulk samples. The TMA data imply that this polymer does not soften appreciably to either a molten or a semimolten phase over the temperature range studied. The initial TGA weight decrease (~350 °C) arises from loss of H_2 caused by cleavage of B–H bonds and concomitant formation of B–B bonds, as inferred from IR studies of the polymer prior to and after the weight change (decrease in intensity of absorption at ~2500 cm^{-1}, relative to other absorptions). Likewise, intermediate weight loss (~550 °C) presumably is due to processes involving cleavage of C–H bonds and concomitant formation of B–C bonds. High-temperature weight loss (>1000 °C) is associated with removal of phosphorus and oxygen. A detailed description of the pyrolysis mechanism for the $[-B_{10}H_{12}\cdot Ph_2POPPh_2]_x-$ polymer to ceramic conversion is beyond the scope of the data available at this time.

Between 1000 and 1500 °C, both powder and bulk samples exhibit the same weight losses as the average rate followed by the bulk samples from room temperature to 2350 °C. This trend is consistent with the loss of the last element-hydrogen moieties, observed in DRIFT data (above). Unfortunately, there is a gap in the TGA data for the bulk samples arising from sample size limitations in the low-temperature TGA. The total weight loss for bulk samples between 1500 and 2350 °C corresponds closely to that predicted for the complete loss of the phosphorus and oxygen still present in the material at 1500 °C. The agreement between the room-temperature, 1000 °C, and 1500 °C data points for the powder and bulk samples suggests that the two sample types behaved similarly between room temperature and 1000 °C. However, surface area results discussed below indicate the potential for differences. Below 1000 °C, shrinkage of the bulk samples occurs at two specific temperature levels (250 and 850 °C) which do not coincide precisely with temperatures where weight losses are concentrated in the powder samples. Above 1000 °C, bulk shrinkage persists at a reduced rate.

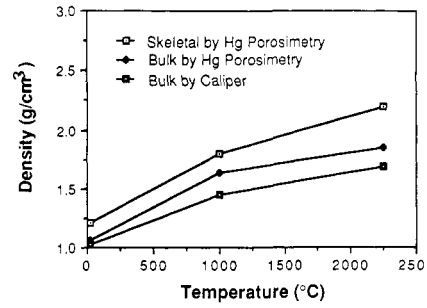

Figure 5. Graph of density of the material produced by pyrolysis of the $[-B_{10}H_{12}\cdot Ph_2POPPh_2]_x-$ polymer as a function of temperature.

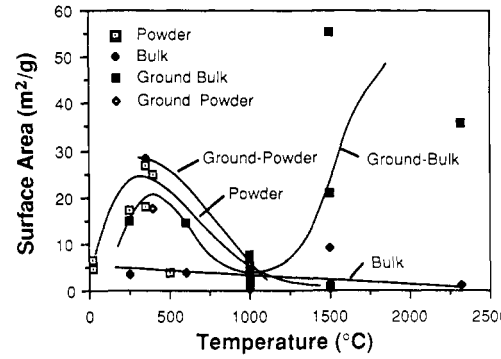

Figure 6. Specific surface areas, measured by the BET method, of bulk, ground bulk, powder, and ground powder samples derived from pyrolysis of the $[-B_{10}H_{12}\cdot Ph_2POPPh_2]_x-$ polymer as a function of firing temperature.

Densities of bulk samples (measured after cooling to ambient temperature by both calipers and Hg porosimetry) increase continuously with firing temperatures up to 2250 °C (Figure 5). The density of the solid phase including closed pores (skeletal density) increases at a higher rate than the bulk density in the temperature range above 1000 °C. All of these density values are subject to error because of the small sample sizes and irregular shapes. However, the trends and relative values are reproducible. At its maximum, the skeletal density (as determined by Hg porosimetry) reaches ~100% of the theoretical value for a B_4C + C body having the overall nominal composition given above.

The results of BET surface area determinations for powder, bulk, ground bulk, and ground powder samples are summarized in Figure 6. These complex results show that materials fired as powder and bulk differ from one another over the entire range of temperatures investigated. Bulk samples exhibit progressively reduced surface areas from 250 °C to the highest temperature studied (2350 °C). The ground bulk samples show that the reduced surface area does not result from conventional densification mechanisms; rather, internal pores become isolated from

(13) Nyquist, R. A.; Kagel, R. O. *Infrared Spectra of Inorganic Compounds*; Academic: New York, 1971.

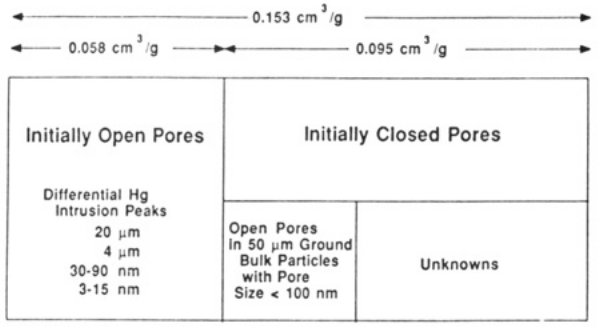

Figure 7. Summary of porosity types found in a sample of the ceramic produced from the $[-B_{10}H_{12}\cdot Ph_2POPPh_2]_x-$ polymer fired in bulk at 1000 °C for 0.5 h. The absolute specific volumes are shown at the top. The results of Hg porosimetry measurements are summarized.

the outer surface. As shown by the ground bulk samples, high-surface-area pores evolve within bulk samples during the initial weight loss up to ~300 °C and then diminish with increasing temperature. Powder, ground bulk, and ground powder samples exhibit similar behavior for temperatures up to ~1000 °C. Surface areas for these three sample types pass through maxima at ~300 °C and then decrease to values exhibited by bulk samples at 1000 °C. Some of the variance between the surface areas of the 1000 °C samples arises from not grinding the samples to the same particle size; the specific area of the ground samples depends on the fraction of total porosity that was exposed to the exterior surfaces of the particles.

For firing temperatures above 1000 °C, the bulk samples show another unusual characteristic. The ground bulk samples reveal that bulk samples again form extremely small, isolated pores at these higher temperatures. BET characterization of the ground bulk samples shows that up to 15% of the initially closed porosity in the bulk samples becomes connected to the exterior surfaces by grinding bulk samples to a particle size of ~50 μm; these pores have a characteristic dimension of less than 100 nm. The total volumes and partition of the pore types in bulk samples after firing to 1000 °C and after grinding (ground bulk) are summarized in Figure 7. These characterizations of the ground bulk samples do not permit estimations either of pores having dimensions greater than 100 nm which are exposed upon grinding or of pores that still remain closed within the ~50-μm particles after grinding.

Channel diameters in the initially open pore structure of bulk samples fired at 1000 °C for 0.5 h were measured by Hg porosimetry; peaks occur at 20 μm, 4 μm, 30–90 nm, and 3–15 nm (Figure 7). SEM photomicrographs show that pores with diameters larger than 2–4 μm result from gross defects (such as entrapment of bubbles or aggregates of several ~5-μm-diameter polymer particles) and that the 30–90-nm pores result from voids, often lenticular, between the original particles that have not completely consolidated by sintering mechanisms. Presumably, these gross defects could be removed by exerting improved control over process variables. The 3–15-nm features probably result from a pore structure that evolves during pyrolysis. The pore size distribution (by number, observed by SEM) on a fracture surface of a 1000 °C bulk sample peaked at nominally 100 nm.

The pore size distribution determined by N_2 adsorption of a bulk sample fired at 1000 °C for 0.5 h revealed pore radii concentrated in two populations that peaked at ~1.5 nm (9% of measured open porosity) and 30 nm (41%). The total open porosity was 8% of the bulk volume. A 2250 °C sample had only 2% open porosity consisting of the smaller characteristic dimension (2–3 nm) pores. These

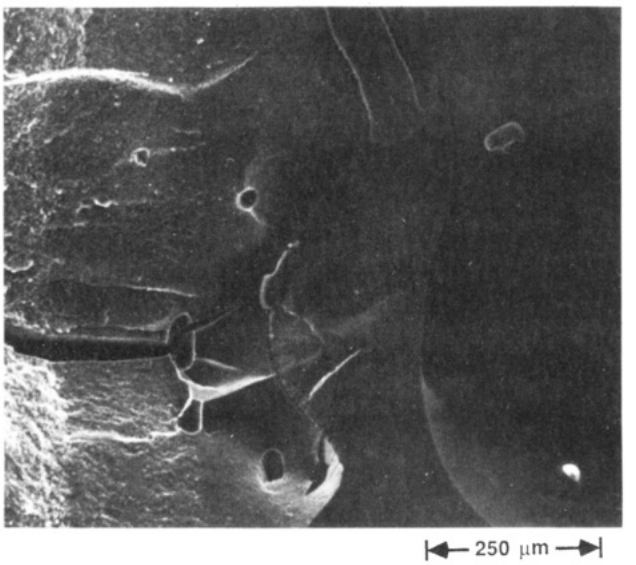

Figure 8. SEM micrograph of a sample of the ceramic derived from the $[-B_{10}H_{12}\cdot Ph_2POPPh_2]_x-$ polymer fired in bulk at 1500 °C for 25 h illustrating crack damage originating from an isolated pore.

nitrogen adsorption results agree with the SEM and Hg porosimetry results. TEM micrographs of bulk samples fired at 1500 °C for 10 h reveal features that resemble high number density, spherical pores having ~2-nm diameters. It still must be verified that these features are not damage that resulted from ion thinning.

Much of the weight loss from the $[-B_{10}H_{12}\cdot Ph_2POPPh_2]_x-$ polymer occurs after pores become isolated in bulk samples, whereas pores within the smaller diameter powder samples retain pathways to the exterior surfaces. Isolation of pores before gaseous products have completely escaped presents obvious problems with respect to internal pressures. A photomicrograph of a crack originating from a (presumably isolated) pore within a bulk sample fired at 1500 °C for 25 h is shown in Figure 8. The potential for this type of damage will impose dimensional limits upon parts produced by pyrolysis of fabricated shapes from the $[-B_{10}H_{12}\cdot Ph_2POPPh_2]_x-$ polymer unless firing cycles are identified that do not cause premature closure of pores.

Conclusions

The characterizations described above have demonstrated the feasibility of using the $[-B_{10}H_{12}\cdot Ph_2POPPh_2]_x-$ polymer to produce B_4C-containing material. They also have revealed issues that must be resolved before these materials can compete effectively with conventionally processed bulk materials. Defects in the polymer-derived material include large quantities of free carbon, as well as phosphorus and oxygen residuals, and cracks generated by gas evolution within closed pores. All of these features are much less severe in powder samples, especially those that are amorphous. Thus, intermediate service temperature fibers and coatings are a possible application for this chemistry. The excess carbon may be consumed by the addition of reactive boron to the polymer. Many other feasible chemistries are known, so it is likely that the premature pore closure issue observed with these bulk samples can be controlled with careful processing of alternative chemistries. The extremely small diameter closed porosity should not be a problem for oxidation resistance or mechanical properties.

Experimental Section

General Comments. All manipulations were carried out in

oven-dried glassware under an inert atmosphere (argon or nitrogen) following standard techniques.[14] All solvents were distilled from appropriate drying agents[15] under a nitrogen atmosphere prior to use. Unless otherwise given, all reagents employed were available commercially and were used as received. Twice sublimed decaborane(14) was purchased from Callery Chemical Co., Callery, PA, and used as received. Triethylamine (Aldrich) was distilled from CaH_2 under argon immediately prior to use. Both $B_{10}H_{12}{\cdot}2(Ph_2PCl)$ and $B_{10}H_{12}{\cdot}2(Ph_2POH)$ were prepared and checked for purity by melting-point analysis (206–208 °C, lit.[16] 212 °C, and 212–215 °C softening, lit.[16] 216 °C softening, respectively). Boron carbide powder (99.5%, <5 μm) was purchased from Cerac and dried at 130 °C for 15 h.

NMR spectra were obtained by using a Varian XL-300 NMR spectrometer, IR spectra on a Perkin-Elmer Model 1430 spectrophotometer. Ceramic analyses were obtained from Galbraith Laboratories, Knoxville, TN, and C and H analyses on nonceramic materials were obtained from Scandinavian Microanalytical Laboratory, Herlev, Denmark. Qualitative content and spatial distribution for phosphorus were determined by using an EG&G Ortec System 5000 EDS attached to a Hitachi S-530 SEM and a Linc LZ5 Series E windowless EDS detector attached to a VG HB5 STEM, respectively.

A hardened stainless steel die was used for forming 1.5 in. × 0.5 in. bars. A Carver laboratory press was used for bar formation. Isostatic bar compaction was carried out in a pneumatically driven oil press with the bars wrapped in Saran Wrap and contained in evacuated, sealed rubber bags. Lindberg tube furnaces with Eurotherm controllers were used for all preparative scale (>1 g) pyrolyses (powder and bulk) to 1500 °C. For pyrolyses to 1000 °C, 1.5-in. o.d. quartz tubes and fused silica boats were used for all samples; for those to 1500 °C, 2.5-in. o.d. mullite tubes and boron nitride boats supported on alumina dee tubes were used; for those to 2350 °C a 1.1-in. o.d. graphite tube furnace and vitreous carbon boats were used. All pyrolyses were carried out under an atmosphere of flowing argon. For experiments to 1000 °C the flow rate was ~6–8 L/h, for experiments to 1500 °C it was ~16–20 L/h, and for experiments to 2350 °C it was ~50–70 L/h.

DRIFT spectra were recorded on an IBM Model IR/85 spectrophotometer. X-ray diffraction patterns were obtained either on a Charles Supper detector and Diano generator instrument or on a Rigaku rotating-anode system. SiC grinding wheels were used to expose internal cross sections of bars for X-ray diffraction.

TMA and TGA measurements were made on a Perkin-Elmer model TGS2 instrument equipped with a Thermal Analysis System 4 controller. In situ TMA data were gathered from ambient temperature to 350 °C; from 350 to 2350 °C measurements were performed on samples that had been heated to the desired temperature and then cooled to ambient. For TGA data, in situ data were obtained for powdered samples from ambient to 950 °C, and mass change data for higher temperatures were collected on bulk samples after they had been heated to the desired temperature and then cooled to ambient conditions. Bulk densities were calculated by using sample mass and caliper-determined volumes. Bulk and skeletal densities as well as pore size distributions were determined by using a Micromeritics Autopore 9220 porosimeter.

Nitrogen adsorption was employed for surface area measurement, as well as an alternative technique for pore size determination. A Quantachrome Quantasorb surface area analyzer and an Omicron Technology Omnisorp 360 instrument were used, respectively, in these adsorption measurements. Powder and bulk samples were characterized as prepared. Bulk samples were broken into pieces consistent with the instrument capacity. Ground bulk and ground powder samples were obtained by grinding bulk and powder samples, respectively, by using an alumina mortar and pestle for about 15 min, until the powder appeared to be uniform. Pore characteristics also were observed by electron microscopy on fractured or polished specimen surfaces.

Phases and grain sizes were studied by STEM and TEM microscopy and by XRD. A JEOL 200CX instrument was utilized for all TEM and STEM measurements. Two methods were used for TEM sample preparation. Beginning with a thin slice of a ceramic bar, a concave surface was ground into the sample; then it was argon ion milled. The center was perforated to give a circle of the appropriate thickness needed for observation. Alternatively, a bulk sample was powdered, and the resultant powder was deposited on a thin carbon film by dipping the film into a dispersion of the powder in hexane.

Preparation of $[-B_{10}H_{12}{\cdot}Ph_2POPPh_2]_x-$.[7a] To a suspension of 27.74 g (0.05 mol) of $B_{10}H_{12}{\cdot}2(Ph_2PCl)$ and 25.92 g (0.05 mol) of $B_{10}H_{12}{\cdot}2(Ph_2POH)$ in 250 mL of benzene was added dropwise with stirring, under nitrogen, a solution containing 10.12 g (0.10 mol) of Et_3N in 250 mL of benzene. After addition was complete, the solution was stirred at reflux for 1 h, cooled to ambient temperature, and filtered in air. The off-yellow solid was washed with 2 × 100 mL of 0 °C acetone, 5 × 100 mL of water, and 5 × 100 mL of 50 °C acetone to give a white powder. Drying for 15 h at ambient temperature and 0.01 mmHg gave 29.14 g (58%) of a free-flowing powder, mp >360 °C. The TGA (to 950 °C at 10 °C/min, argon atmosphere) showed a ceramic yield of 93%. Anal. Calcd for $C_{24}H_{32}OP_2B_{10}$: C, 56.89; H, 6.37. Found: C, 55.94; H, 6.08. $^{11}B\{^1H\}$ NMR (DMSO) 70–30, 24, 18 to −10, −24 to −42 (all br) ppm. $^{31}P\{^1H\}$ NMR (DMF-d_7) 69–72 (br) ppm. $^{13}C\{^1H\}$ NMR (DMF-d_7) 129, 133 ppm (ipso C not observed). ^1H NMR (DMF-d_7) 7.3–8.2 (br, C_6H_5) ppm. IR (nujol) 2540 m, 2520 s, 2500 m, 1376 s, 1110 s, 1005 m, 980 w, 960 s, 914 m, 875 w, 785 w, 742 m, 718 m, 688 m, 641 w cm^{-1}.

Pyrolysis of $[-B_{10}H_{12}{\cdot}Ph_2POPPh_2]_x-$. A 1.09-g sample of the powdered polymer was placed in two fused silica boats and heated in a quartz tube, under an atmosphere of flowing argon, to 1000 °C at a rate of 10 °C/min, held at 1000 °C for 0.5 h, and allowed to cool to ambient temperature over a period of ~3.5 h. The powdery black residue, 0.937 g (86%), which had shrunk ~24% from the sides of the boat, was amorphous by XRD and had DRIFT absorptions at 2350–3100 and 1104–1406 cm^{-1}, with maxima at 1190 and 1302 cm^{-1}. Anal. Found: B, 23.67; H, 0.2; C, 57.40; P, 11.54. A 0.336-g powder sample of this pyrolysis product was placed in a boron nitride boat and heated in a mullite tube, under an atmosphere of flowing argon, to 1000 °C at a rate of 25 °C/min, held for 1 h at 1000 °C, heated to 1500 °C at a rate of 10 °C/min, held for 10 h at 1500 °C, and cooled to ambient temperature over a period of ~10 h. The residue, 0.274 g (82%), had not visibly changed in appearance; however, a yellow/orange film had deposited on the walls of the pyrolysis tube. Broad diffractions at d = 3.8 and 2.5, indicative of a weakly crystalline material, were observed for B_4C by XRD (JCPDS 35-798, B_4C: d = 2.38, 2.56, 3.78). DRIFT absorptions were present at 1560–1580, 1090–1105, and 780–830 cm^{-1}. Anal. Found: B, 28.9; C, 60.2; P, 0.39; O, 2.88.

Pyrolyses of bulk samples to higher temperatures gave the following results: to 1500 °C, B, 25.16; C, 55.42; P, 11.22; O, 6.66; to 2350 °C, B, 29.15; C, 65.14; P, nil.

General Procedure for the Preparation of Ceramic Composite Bars Using $[-B_{10}H_{12}{\cdot}Ph_2POPPh_2]_x-$ Polymer as a Binder for Boron Carbide Powder. Weighed quantities of $[-B_{10}H_{12}{\cdot}Ph_2POPPh_2]_x-$ (0.5 g) and B_4C powder (2.5 g) were mixed and ground for 15 min in an alumina mortar and pestle in an inert-atmosphere box. The samples thus prepared were placed in a 0.5 in. × 1.5 in. rectangular die and formed into bars in a Carver laboratory press at 5000 pounds (6667 psi uniaxially), removed to an ambient temperature isostatic press and further compacted to 50 000 psi after being wrapped in Saran Wrap and placed in an evacuated, sealed rubber bag. The uniaxial pressing time duration was ~5 min, and the isostatic pressing time duration was ~15 min. The resulting bar was pyrolyzed in a stream of argon to 1000 °C (10 °C/min heating rate, hold at 1000 °C for 30 min) and allowed to cool to ambient temperature over a period of ~3.5 h. The pyrolyzed sample was handled in an inert-atmosphere box.

For the purposes of this initial screening, a ceramic bar was considered to be "excellent" if it was a uniform, black rectangular monolithic body that had retained its shape (vs the polymer bar before pyrolysis) in all three dimensions without undergoing any

(14) Shriver, D. F.; Drezdzon, M. A. *Manipulation of Air Sensitive Compounds*, 2nd ed.; Wiley: New York, 1986.
(15) Gordon, A. J.; Ford, R. A. *The Chemist's Companion*; Wiley: New York, 1977.
(16) Schroeder, H. A.; Reiner, J. R.; Heying, T. L. *Inorg. Chem.* **1962**, *1*, 618.

discernible shrinkage or bloating above the detectable level of 3-5% and if its strength was such that it could not be broken manually without employing the aid of mechanical means (e.g., a vise and pliers). Such a composite bar prepared by using the $[-B_{10}H_{12}\cdot Ph_2POPPh_2]_x-$ polymer as a binder for B_4C powder was classified as excellent.

Procedure for the Preparation of Ceramic Bars from the $[-B_{10}H_{12}\cdot Ph_2POPPh_2]_x-$ Polymer. A 3.0-g sample of the polymer was finely powdered for 15 min in an alumina mortar and pestle in an inert-atmosphere box and then placed in a 0.5 in. × 1.5 in. rectangular die. Uniaxial pressing in a Carver press to 5000 pounds (~5 min) was followed by ambient temperature isostatic compaction at 50 000 psi (~15 min). The polymer bar thus obtained had the approximate dimensions 0.5 in. × 1.5 in. × 0.25 in.

The weighed and micrometer-measured polymer bar was introduced into a fused silica pyrolysis boat that then was inserted into a quartz tube that had been flushed with argon for 15 min and the end of the tube was connected to an oil bubbler. After ~5 min, the argon flow was reduced from ~100 mL/min to ~20-30 mL/min, and the quartz tube was placed in a Lindberg tube furnace and heated at a rate of 10 °C/min to a temperature of 1000 °C, held at 1000 °C for 0.5 h, and allowed to cool to ambient temperature over a period of ~3.5 h. The ceramic bar was removed to an inert-atmosphere box, weighed, micrometer measured and then subjected to further evaluation or transferred to the appropriate furnace for temperature treatment above 1000 °C. Heating rates for temperatures to 1500 °C were 25 °C/min. For temperatures above 1500 °C, the heating rate was 17 °C/min.

Preparation and Processing of a Boron Powder/$[-B_{10}H_{12}\cdot Ph_2POPPh_2]_x-$ Polymer Mixture. The average values of boron [(23.7 + 28.9)/2] and carbon [(57.4 + 60.2)/2] found in the 1000 and 1500 °C samples of fired $[-B_{10}H_{12}\cdot Ph_2POPPh_2]_x-$ polymer powder, 26.3 and 58.8, respectively, were used to calculate the necessary amount of boron required to provide a theoretical boron/carbon ratio of 4/1. Thus, a mixture of 0.80 g of $[-B_{10}H_{12}\cdot Ph_2POPPh_2]_x-$ polymer and 1.40 g of amorphous boron powder (Cerac, 94%, <5 μm) were mixed in an alumina mortar and pestle in an inert-atmosphere box for 15 min. A 2.00-g sample of this mixture pyrolyzed to 1000 °C resulted in 1.83 g (92%) of an amorphous, dull gray-black powder. Anal. Found: B, 73.23; C, 21.34; P, 4.18. Further heating to 1500 °C of 0.512 g of the material thus produced gave 0.476 g (7% weight loss from 1000-1500 °C; overall yield to 1500 °C, 85%) of a metallic, silver-black powder containing crystalline B_4C. Anal. Found: B, 76.88; C, 18.00; P, 2.58.

Acknowledgment. This work was supported by Contract No. N00014-85-K-0645 (SDIO/IST). Materials characterizations of all types were carried out by Jason Lewis, a participant in the Undergraduate Research Opportunities Program (UROP). Professor Lisa Klein of Rutgers University corroborated our N_2 adsorption and pore volume measurements.

Selective Syntheses of FeTe and $FeTe_2$ from Organometallic Precursors. Synthesis and Pyrolysis of $[Cp(Et_3P)(CO)Fe]_2(Te)_n$

M. L. Steigerwald

AT&T Bell Laboratories, Murray Hill, New Jersey 07974

Received June 27, 1988

We have devised selective syntheses of the solid-state compounds FeTe and $FeTe_2$ using organometallic reagents. Bis(dicarbonylcyclopentadienyliron) reacts with either 1 or 2 equiv of triethylphosphine telluride in the presence of excess phosphine to give $[Cp(Et_3P)(CO)Fe]_2Te$, **1**, and $[Cp(Et_3P)(CO)FeTe]_2$, **2**, respectively. Each compound is stable, crystalline, and easily purified. Each is a mixture of diastereomers as shown by ^1H, ^{31}P, and ^{125}Te NMR spectroscopies. That **1** is an intermediate in the synthesis of **2** is shown by independent reaction of **1** with Et_3PTe to yield **2**. That this reaction is reversible is shown by removal of Te from **2** with Et_3P to give **1**. Low-temperature pyrolysis of **1** gives FeTe and of **2** gives $FeTe_2$, and each of these is specific with respect to solid-state product. Along with CO and Et_3P, ferrocene is produced quantitatively in these pyrolyses. These reactions demonstrate that (1) low-temperature preparation of solid-state compounds is possible using fairly complicated organometallic precursors, (2) product selectivity can be ensured by a proper choice of precursor, and (3) particularly stable organometallic leaving groups such as ferrocene are advantageous both by driving the pyrolysis and by conveniently removing unwanted organic residue.

Introduction

The syntheses of inorganic solid-state compounds are most typically achieved by combination of the proper stoichiometries of the elements as solids.[1] So that complete interdiffusion of the solid reagents may be ensured, these reactions are usually run at high temperature; however, this can be a severe limitation. Lower processing temperatures allow the isolation of metastable phases and give wider latitude in the fabrication of complicated structures (heterostructures, quantum wells, etc.) which would be unstable at higher temperatures. In part to avoid such harsh reaction conditions, there has been increasing interest in the use of precursor methods.[2] The general technique here is not to combine the elements but rather to combine molecular precursors to the elements such that when the precursors are heated or otherwise chemically treated the ancillary components are removed as the

(1) (a) Schafer, H. *Angew. Chem. (Int. Ed. Engl.)* **1971**, *10*, 43-50. (b) Wold, A. *J. Chem. Educ.* **1980**, *57*, 531-6.

(2) (a) West, A. R. *Solid State Chemistry and Its Applications*; Wiley: New York, 1984; pp 16-31. (b) Rao, C. N. R.; Gopalakrishnan, J. *New Directions in Solid State Chemistry*; Cambridge University Press: Cambridge, UK, 1986; pp 116-24. (c) Foise, J.; Kim, K.; Covino, J.; Dwight, K.; Wold, A.; Chianelli, R.; Passaretti, J. *Inorg. Chem.* **1983**, *22*, 61-3. (d) Pasquariello, D. M.; Kershaw, R.; Passaretti, J. D.; Dwight, K.; Wold, A. *Inorg. Chem.* **1984**, *23*, 872-4. (e) Jensen, J. A.; Gozum, J. E.; Pollina, D. M.; Girolami, G. S. *J. Am. Chem. Soc.* **1988**, *110*, 1643-4. (f) Nanjundaswamy, K. S.; Vasanthacharya, N. Y.; Golabkrishnan, J.; Rao, C. N. R. *Inorg. Chem.* **1987**, *26*, 4286-8. (g) Kisker, D. W.; Steigerwald, M. L.; Kometani, T. Y.; Jeffers, K. S. *Appl. Phys. Lett.* **1987**, *50*, 1681-3. (h) Steigerwald, M. L.; Sprinkle, C. R. *J. Am. Chem. Soc.* **1987**, *109*, 7200.

0897-4756/89/2801-0052$01.50/0